ELSEVIER

Nuclear Physics A 642 (1998) 407–418

NUCLEAR PHYSICS A

Fragment mass distribution of fission after incomplete fusion in the reaction ^{7}Li (43A MeV) + ^{232}Th ⋆

H.-G. Ortlepp [a], W. Wagner [a,1], C.-M. Herbach [a], P. Gippner [a], K.D. Schilling [a], Yu.E. Penionzhkevich [b]

[a] *Forschungszentrum Rossendorf e.V., PF 510119, 01314 Dresden, Germany*

[b] *Joint Institute for Nuclear Research, Dubna, Russia*

Received 12 June 1998; revised 6 August 1998; accepted 9 September 1998

Abstract

Fragment mass distributions of binary fission were measured for the reaction ^{7}Li (43A MeV) + ^{232}Th in dependence on the linear momentum transfer. The excitation energy (E^*) of the compound nuclei produced by incomplete fusion was deduced applying the massive transfer approach and amounted to 57–205 MeV. The analysis procedure avoids distortions due to the acceptance and error correlation. Total fragment masses and single fragment mass dispersions are discussed in terms of E^*, temperature and an effective parameter describing the stiffness against mass asymmetry. Assuming unchanged stiffness, the dispersions at E^* in excess of $\approx$ 70 MeV are found to be considerably smaller than expected. This behaviour is interpreted as a consequence of the remarkable cooling down of the hot nuclei due to neutron emission before the fragment masses are formed in the course of fission. Agreement with the data is achieved supposing a cooling time of $(60 \pm 20) \times 10^{-21}$ s based on the neutron emission time taken from the statistical model. It is concluded that fission remains a relatively slow process up to excitation energies of about 200 MeV. © 1998 Elsevier Science B.V.

PACS: 25.70.Jj

Keywords: NUCLEAR REACTIONS ^{232}Th(^{7}Li, F), E = 43 MeV/nucleon; measured binary fission fragments mass, energy distributions; deduced compound nucleus cooling time, fission dynamics.

⋆ Supported by the BMBF, Germany, under contract 06 DR 671.

[1] Corresponding author. E-mail: W.Wagner@FZ-Rossendorf.de

0375-9474/98/$ - see front matter © 1998 Elsevier Science B.V. All rights reserved.
PII S0375-9474(98)00491-6

1. Introduction

Nuclear fission is one of the dominating decay modes of heavy nuclei for a large interval of excitation energy (E^*). At $E^* > 50$ MeV the fission process is characterized by transient times depending on the dynamics of this collective motion of nuclear matter [1]. The evolution of fission at even higher E^* is a problem raising several interesting questions.

According to Ref. [2] (and references therein) the fission fragment mass dispersion (σ_m) can be related to a temperature (Θ) and the stiffness (q) of the fissioning system against mass asymmetry

$$\sigma_m^2 = \frac{\Theta}{q}. \tag{1}$$

For sufficiently massive systems ($Z^2/A > 33$) the liquid drop model (LDM) predicts an increasing stiffness along the descent from the saddle to the scission point. Compiled in Ref. [3], it amounts for nuclei around Th to $q_{\mathrm{sad}} < 0.003$ MeV/amu^2 at the saddle and $q_{\mathrm{sci}} > 0.010$ MeV/amu^2 near scission. Regardless of some small differences in the absolute numbers, this general trend commonly holds to the predictions made by different LDM versions [4,5] or the droplet model [6]. Already in the late 60's it has been established that the experimentally found variances of the fragment mass distributions of heavy systems cannot be reproduced neither by q_{sad} nor by q_{sci}. A satisfactory description of σ_m by Eq. (1) for E^* up to about 100 MeV could be achieved by the introduction of an effective stiffness parameter (q_{eff}) phenomenologically accounting for the saddle-to-scission transition [7].

A further question concerns the damping of the mass-asymmetry degree of freedom during the descent from the saddle to scission. Measurements of scission times showed that the collective motion along the elongation coordinate is overdamped [1,8,9] and fission is a relatively slow process. If the relaxation time for the motion in direction to mass asymmetry is small compared with the saddle-to-scission transient time, then Eq. (1) applies, and σ_m should be governed by the Θ near scission and q_{sci}. Otherwise a more general description of σ_m for fission of hot nuclei in a multi-dimensional dynamical treatment is required.

Presently, there exist different dynamical approaches following the Langevin [10,11] or the Fokker–Planck [3,12] formalism. A review of different stochastic approaches applied to fission dynamics is given in Ref. [13]. For the first time, fission fragment mass distributions were calculated by the use of a three-dimensional Langevin simulation in Ref. [14]. Predictions of σ_m in terms of q_{eff} [2] for the large variety of measured data at $E^* = 50$–100 MeV, however, are available up to now only from calculations using the model of Ref. [3].

As is known from the measurements of pre- and post-scission neutrons [1,8], at higher initial E^* the system cools down considerably during its evolution towards scission, but an open question is which temperature is decisive for the formation of the mass distribution. In this consideration, the precise measurement of σ_m at $E^* > 100$ MeV should

give substantially new insights. This is, however, by no means a simple experimental task, mainly because of the following two reasons:

(i) Binary reaction mechanisms like deep inelastic collisions or fast fission, which bypass a hot and little-deformed compound system, have to be excluded effectively.

(ii) Fluctuations of the transferred transversal momentum as well as the cumulative recoil from evaporated particles can smear out the kinematic correlation between the fission fragments basically used by the kinematic coincidence methods [15,16].

2. Experimental set-up

The present measurement has been carried out on a heavy-ion beam of the isochronous cyclotron U-400M [17] of the JINR in Dubna. We chose the very asymmetric reaction ^{7}Li + ^{232}Th, where sufficiently massive fragments can arise only from the decay of a compound nucleus. A thin (240 μg/cm^2) target of ^{232}Th deposited on an Al_2O_3 backing (40 μg/cm^2) was positioned in the centre of the 4π fragment spectrometer FOBOS [18]. The intensity of the ^{7}Li beam amounted to 2×10^9 ions per second.

The experiment was originally devoted to the investigation of fission accompanied with a third fragment of intermediate mass [19]. The present analysis, however, considers only binary events recorded by two opposite FOBOS modules [18] positioned at the polar angles (ϑ) of 37° and 143° relative to the beam axis at a distance of 54 cm from the target. Each module consisted of a position sensitive avalanche counter and an axial ionization chamber covering 36° of opening angle. One small transmission avalanche counter was mounted near the target at ϑ = 37° and delivered the timing reference signal for fission fragments within its effective solid angle.

3. Data analysis

From the measured quantities of the fragments—the coordinates (ϑ, φ), the time-of-flight (TOF), and the residual energy (E)—the individual fragment masses (m_1, m_2) and momentum vectors (p_1, p_2) were derived "event by event" applying the TOF-E method without any kinematical assumption. The calibration procedure and the corrections made for energy losses in the detector window foils are described in Refs. [18,20]. The correction of the TOF, necessary in the case if only one reference detector is used to trigger both fission fragments, was taken into account.

Further essential quantities—the transferred linear momentum (p_{trans}), the folding angle, the mass and momentum vector sums ($\sum m_i$, $\sum p_i$; $i = 1, 2$), the relative velocity of the fission fragments, and the c.m. velocity vector of the fissioning system (v_Σ)—were determined for each fission event. Some preliminary qualitative results concerning the width of the fission fragment mass distribution in relation to the transferred linear momentum have already been published in Refs. [20,21]. Meanwhile the same raw data body has been analysed in a more complex way to deduce the dependency of the

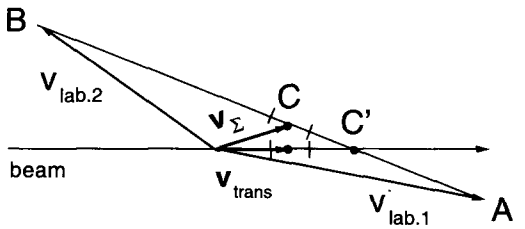

Fig. 1. Velocity diagram of the reaction investigated. The fission fragment velocities $v_{\mathrm{lab.1}}$ and $v_{\mathrm{lab.2}}$ are measured. At scission the fissioning nucleus moves with the velocity v_Σ not identical with the initial $v_{\mathrm{c.m.}}$ (see text).

fragment mass dispersion of symmetric fission on E^*. Two more aspects are considered in the present work:

(i) the contribution of asymmetric ("last chance") fission at low energy, and

(ii) possible mass–momentum correlations due to accidental errors.

At the bombarding energy of 43A MeV, compound systems with a rather broad spectrum of initial E^* are produced by incomplete fusion [22]. To select those of equal mean E^*, the events have been sorted into discrete bins of transferred linear momentum. The velocity diagram shown in Fig. 1 illustrates the fission kinematics. After incomplete fusion and pre-scission particle evaporation, i.e. just in the instant before scission, the system moves with velocity v_Σ. In this frame the fission fragments have the velocities C–A and C–B. If only $v_{\mathrm{lab.1}}$ and $v_{\mathrm{lab.2}}$ are measured (kinematic coincidence method), the transversal component of v_Σ cannot be determined, and, consequently, the masses (m_1, m_2) derived by the use of the velocities C'–A and C'–B are incorrect. (Therefore we use the symbol v_Σ instead of the conventional one $v_{\mathrm{c.m.}}$.) In our analysis, the mass determination is independent of v_Σ. Furthermore, v_Σ follows directly from the ratio $\sum p_i / \sum m_i$. A sufficiently large value of $\sum m_i$ and a limited deviation of the direction of $\sum p_i$ from the beam axis (< 150 MeV/c) were used as the two criteria for the selection of binary decays.

4. Results and discussion

The distribution of the transferred longitudinal momentum (p_{trans}) determined by the projection of $\sum p_i$ on the beam axis is shown in Fig. 2. A separation of central and peripheral collisions into two distinct peaks of transferred linear momentum (as e.g. observed in Ref. [23] for Ar + Th collisions) does not occur due to the very light ^{7}Li projectile. The broad bump indicates a smooth transition from lower to higher p_{trans}. The maximum at 1100 MeV/c fairly well agrees with the most probable transferred linear momentum predicted in Ref. [24] for central collisions at intermediate energies by a value of 160–180 MeV/c per projectile nucleon.

In the framework of the massive-transfer approximation, the initial excitation energy after incomplete fusion of a very asymmetric system can be estimated by the relation

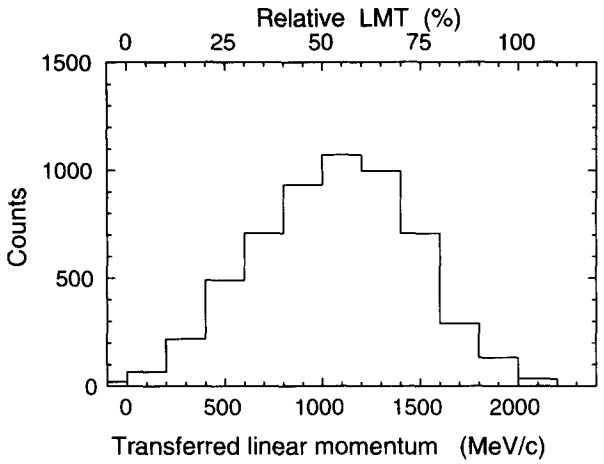

Fig. 2. Distribution of the transferred linear momentum p_{trans} (i.e. the sum of the momentum projections of both fission fragments on the beam axis). The linear momentum transfer (LMT) was calculated by use of Eq. (2).

$$E^* \approx E_{\text{c.m.}} \frac{p_{\text{trans}}}{p_{\text{pro}}}, \tag{2}$$

where $E_{\text{c.m.}}$ indicates the c.m. kinetic energy in the entrance channel, and p_{pro} is the linear momentum of the projectile [23,25].

An accurate evaluation of σ_m as a function of E^* needs to take into consideration the following effect. The mass determination by the TOF-E method has a typical uncertainty of 2–5 amu, which is mainly caused by the errors introduced by the correction procedure for the energy losses of the fragments in the window foils of the detectors. This involves an error of the ratio m_1/m_2 used to find point C in the velocity diagram (schematically indicated in Fig. 1 by bars over point C and also projected on the beam axis). Since the longitudinal component of v_Σ (v_{trans}; by analogy with p_{trans}) is calculated from the balance, its error (bars on the beam axis in Fig. 1) in this way correlates with the errors of the fragment masses. This covariance leads to spurious distortions of the extracted fragment mass spectra depending on E^*. To avoid them in the present analysis, the fission events have been sorted into 5 bins of the folding angle which is determined exclusively by the flight directions of the fission fragments and, therefore, not covariant with the masses. Supported by Monte Carlo simulations, only such fragment emission angles (ϑ, φ) were selected for the different cuts regarding to the folding angle, where the geometrical coincidence efficiency is not influenced by the fragment mass splitting (m_1/m_2). For each ensemble of events ($\approx 10^3$ in a bin), the mean transferred linear momentum ($\langle p_{\text{trans}} \rangle$), both mean single fragment masses ($\langle m_1 \rangle, \langle m_2 \rangle$), the mean sum of both fragment masses ($\langle m_{\text{tot}} \rangle$) as well as the corresponding dispersions were determined (see Tables 1 and 2).

Additionally, the spectra of m_1 and m_2 were added up to get better statistics. (Note that m_1 and m_2 are measured independently by different detector modules!). Then the mean single mass ($\langle m \rangle$) and its dispersion ($\sigma_{\langle m \rangle}$) were determined again. The values

Table 1
Mean value of transferred linear momentum (p_{trans}), its dispersion ($\sigma_{p_{\mathrm{trans}}}$), the mean linear momentum transfer ($\langle LMT\rangle$), the mean excitation energy ($\langle E^*\rangle$), the mean total mass ($\langle m_{\mathrm{tot}}\rangle$) with its dispersion ($\sigma_{\langle m_{\mathrm{tot}}\rangle}$) and both mean single fragment masses ($\langle m_1\rangle, \langle m_2\rangle$) for events selected into 5 equidistant bins of the folding angle between 179.5° and 167°. The mean fragment mass ($\langle m\rangle$) was determined from the sum of the spectra of both fragments. $\langle E^*\rangle$ was calculated by use of Eq. (2)

Bin (MeV/c)	$\langle p_{\mathrm{trans}}\rangle$ (MeV/c)	$\sigma_{p_{\mathrm{trans}}}$ (%)	$\langle LMT\rangle$ (MeV)	$\langle E^*\rangle$ (amu)	$\langle m_{\mathrm{tot}}\rangle$ (amu)	$\sigma_{\langle m_{\mathrm{tot}}\rangle}$ (amu)	$\langle m_1\rangle$ (amu)	$\langle m_2\rangle$ (amu)	$\langle m\rangle$
1	405	265	20.3	57	228.5	7.0	112.9	115.0	114.0
2	705	258	35.2	99	225.0	7.2	111.5	112.9	112.2
3	994	244	49.7	139	221.6	7.1	109.0	112.0	110.5
4	1254	250	62.7	175	219.6	7.2	108.8	110.2	109.5
5	1461	271	73.1	205	217.1	7.0	108.3	108.3	108.3

Table 2
Fission fragment mass dispersions (σ in amu) for the same groups of events as given in Table 1 (columns 2–4); $\sigma_{m\,\mathrm{corr}}$ – corrected for resolution. The contribution of asymmetric fission to $\sigma_{m\,\mathrm{corr}}$ at the lowest E^* was suppressed (*) by a TKE cut (Fig. 4). Different estimates (see text) are given in columns 6–8: $\sigma_{q_{\mathrm{eff}}}$ – extrapolation of the systematics of Ref. [2]; σ_{presad} – corrected for pre-saddle neutron emission; σ_{sci} – assuming a LDM prediction for q near scission and that part of E^* remaining at scission

Bin	σ_{m_1}	σ_{m_2}	$\sigma_{\langle m\rangle}$	$\sigma_{m\,\mathrm{corr}}$	$\sigma_{q_{\mathrm{eff}}}$	σ_{presad}	σ_{sci}
1	15.2	15.2	15.3	12.9 *	13.9	–	9.5
2	14.1	13.8	14.0	13.6	16.2	15.8	9.9
3	13.5	13.0	13.4	13.0	17.8	17.0	10.3
4	14.6	14.0	14.3	13.9	19.0	18.1	10.6
5	16.0	15.1	15.6	15.3	19.8	18.8	10.8

obtained for $\langle m_1\rangle$, $\langle m_2\rangle$ and $\langle m\rangle$ agree within 3 amu, which confirms the consistency of the analysis procedure.

The width of the distribution of $\langle m_{\mathrm{tot}}\rangle$ amounts to half the width of the single fragment mass spectra. The decrease of $\langle m_{\mathrm{tot}}\rangle$ with increasing transferred linear momentum (Fig. 3) correlates with the enhancement of particle evaporation. The slope of the dependency $\langle m_{\mathrm{tot}}\rangle$ versus E^* corresponds to an energy of 13.2 MeV per evaporated nucleon. This value is in agreement with the result of a direct measurement of the multiplicity of evaporated particles [26], giving proof of the accurate mass scale deduced. It is crucial for the subsequent analysis to avoid possible systematic distortions of the fragment mass spectra.

The dispersion $\sigma_{\langle m_{\mathrm{tot}}\rangle}$ is used to estimate the upper limit of the mass resolution of our spectrometer by a value of $\leqslant 5$ amu. This response leads to an enlargement of the measured single fragment mass dispersions by about 0.4 amu with respect to the primary ones. The dispersions corrected for resolution ($\sigma_{m\,\mathrm{corr}}$) are given in column 5 of Table 2, and the value of 0.4 amu was taken as the systematic error of σ_m. Since the statistical uncertainty is at least twice as small it has been neglected.

At small transferred linear momenta (or low E^*), contributions from asymmetric

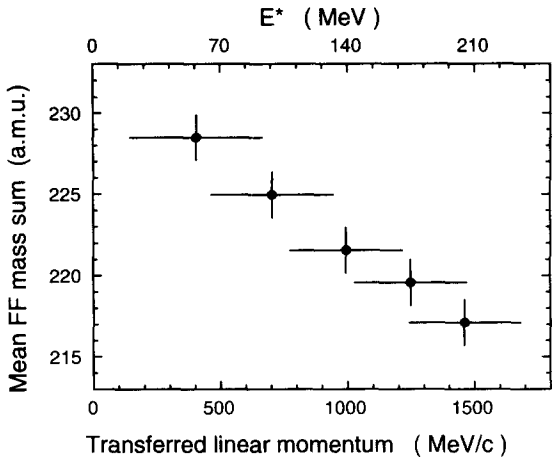

Fig. 3. Mean fission fragment (FF) mass sum ($\langle m_{\mathrm{tot}} \rangle$) versus the transferred linear momentum (p_{trans}). The corresponding excitation energy (E^*) was calculated by use of Eq. (2). The widths of the distributions of the transferred linear momentum for the fission events within the corresponding bin of the folding angle are indicated by horizontal bars. The estimated systematic errors are given as vertical bars.

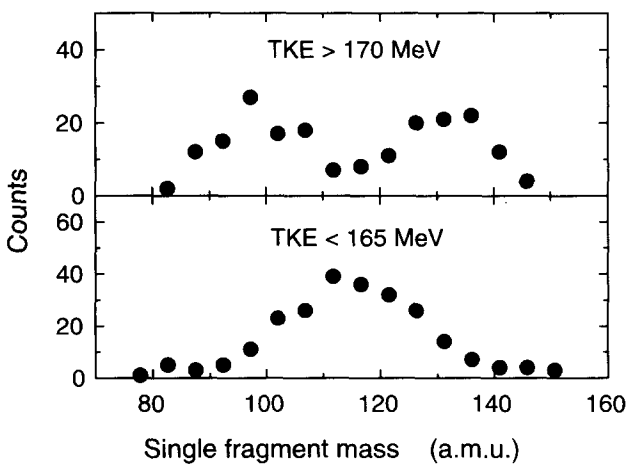

Fig. 4. Fragment mass spectra of fission events at low transferred linear momenta for two cuts of the total kinetic energy (TKE). At small TKE (lower panel) the double-humped component is suppressed. The symmetric component was fitted by a Gaussian between 95 amu and 135 amu.

("last chance") fission influence the dispersion of the fragment mass spectra. The decomposition of the measured fragment mass distribution into a symmetric and an asymmetric component is illustrated in Fig. 4. A double-humped mass spectrum is observed at total kinetic energies (TKE) of the fission fragments larger than 170 MeV. At smaller TKE, contributions of the asymmetric component are suppressed, and the dispersion resulting from a Gaussian fitted to these data is used for the further analysis (see Table 2). A similar decomposition was done in Ref. [27] for the fission of the nucleus ^{224}Th, i.e. of a comparable system, produced by the reaction ^{16}O + ^{208}Pb at a beam energy of 108 MeV. The initial excitation energy reached in this case nearly

corresponds to the lowest E^* of our measurement. The authors of Ref. [27] did not apply TKE cuts, but approximated the mass distribution by either one Gaussian or three Gaussians with given mean masses. Our value of $\sigma_{\langle m \rangle} = 15.3 \pm 0.4$ amu measured at the lowest E^* (bin 1 in Table 2) well agrees with the dispersion of 15.2 amu obtained in Ref. [27] for the approximation by one Gaussian. Unfortunately, dispersions of the three-component fit are not given in Ref. [27].

At sufficiently large transferred linear momenta (or higher E^*), we did not find significant differences in the fragment mass spectra for different TKE cuts, which might be an indication of some asymmetric contribution. Hence, we assumed that there exists only one symmetric component. The measured and resolution-corrected dispersions as well as estimations using Eq. (1) are compiled in Table 2.

5. Interpretation of the observed mass dispersions and conclusions

At $E^* \geqslant 100$ MeV, the deduced dispersions ($\sigma_{m\,\mathrm{corr}}$ in column 5 of Table 2) are up to 40% smaller than predicted by Eq. (1) ($\sigma_{q_{\mathrm{eff}}}$ in column 6 of Table 2) assuming $q_{\mathrm{eff}} = 0.0077$ MeV/amu^2 and

$$\Theta^2 = (E^* - 7\ \mathrm{MeV})/a \tag{3}$$

with a level density parameter $a = A/10$ MeV^{-1} like in Ref. [2]. Since some experimental error which could cause such a substantial reduction of σ_m seems to be most unlikely, the reason for these facts should be of physical nature.

Indeed, the uncertainty of the q_{eff} systematics [2] does not exceed 15%, contributing to the mass dispersion by less than 7.5%. Furthermore, possible angular momentum effects should only lead to a broadening of the mass distribution. Calculations [28] made by using the Boltzmann–Uehlig–Uhlenbeck model with the numerical implementation of Bauer [29] showed that the mean angular momentum transferred in our reaction does not exceed $25\hbar$. The value of q_{eff} given above corresponds to an angular momentum equal to zero. Since, in the region of Th nuclei q_{eff} decreases with increasing angular momentum (see Ref. [30] and references therein), angular momentum transfer can affect σ_m by only 2 amu—but in the "opposite direction" than observed.

The q_{eff} systematics used here [2] relies on data taken at excitation energies smaller than 100 MeV. The temperature responsible for the excitation of the mass-asymmetry degree of freedom there really depends on E^* as given by Eq. (3). In the following discussion we shall assume that the stiffness against mass asymmetry remains unchanged (or decreases by only a small amount) at $E^* \geqslant 100$ MeV. This allows us to draw a first conclusion, namely, that the excitation energy determining σ_m in this region (E_f^*) must be considerably lower than the initial E^* (for more clarity indicated in the following by E_0^*). The loss of excitation energy of the compound system is mainly governed by the evaporation of neutrons. Supposing this process to proceed during the time the system moves towards a stage where the fission fragments are formed (i.e. the primary fragment mass distribution is "frozen out"), we shall, in the following, try different

assumptions to estimate E_f^*, and then put E_f^* instead of E_0^* into Eq. (3) to calculate "energy-corrected" fragment mass dispersions by Eq. (1).

(i) The energy loss by pre-saddle neutron emission is accounted for in column 7 of Table 2, making use of the calculations given in Ref. [31]. The existing experimental data of the pre-saddle neutron multiplicity ($\langle n_{\rm pre}\rangle$) of ^{224}Th could be explained assuming a relatively large constant of the reduced friction ($\beta = 20 \times 10^{21}$ s^{-1}). From the slope of the curve $\langle n_{\rm pre}\rangle$ versus E^* (cf. Fig. 4b in Ref. [31]), we estimated that about two supplementary pre-saddle neutrons are emitted if E_0^* rises from 100 MeV to 200 MeV. Even with this number, assuming a mean energy loss per emitted neutron of ε_n = 14 MeV, the fragment mass dispersions corrected for the pre-saddle neutron multiplicity ($\sigma_{\rm presad}$ in Table 2) remain well above the experimental values $\sigma_{m\,\rm corr}$. Hence, one is led to the conclusions that first the mass distribution of the fission fragments at $E_0^* > 100$ MeV is determined "well after" the instant the pre-saddle neutrons were emitted, and secondly, that more than the pre-saddle neutrons had to be emitted before the system eventually disintegrated by fission. The latter case is consistent with the relation $E_f^* < E_0^*$ already supposed above.

(ii) To calculate the values of $\sigma_{\rm sci}$ (see column 8 of Table 2), the extremely opposite assumption to (i) was made, namely, that the fragment mass distribution is determined just near scission. From the systematics given in Ref. [1], a simple approximation can be derived for the excitation energy of the system remaining at scission: $E_{\rm sci}^* \approx 0.15E_0^* + 30$ MeV. Considering the large LDM value of $q_{\rm sci} = 0.011$ MeV/amu^2 near scission [3], the strong release of energy with respect to E_0^* results in too small mass dispersions compared with the measured data. From fission fragment spectroscopy at low E^* (see Refs. [2,3] and references therein) it is known that the mass distribution of the fission fragments is formed "well before" scission. The estimates made for $\sigma_{\rm sci}$ would mean that these facts hold at higher E_0^* too.

(iii) Therefore it seems to be reasonable to keep the assumption that the fragment mass dispersion at E_0^* = 100–200 MeV is governed by the same effective stiffness $q_{\rm eff} = 0.0077$ MeV/amu^2 as found at lower E^*. We, furthermore, want to introduce some time interval ($t_{\rm del}$) during which the system cools down before it reaches an energy E_f^* determining σ_m. For a given initial $E_0^* = E^*(t_0)$, we intend to find some mean $E_f^* = E^*(t_0 + t_{\rm del})$ based on the mean emission time (τ_n) of one neutron at given E^* [32] and on a value of ε_n = 14 MeV [26]. The cumulative time (t_n) for the emission of a number of n neutrons then reads

$$t_n = \sum_{i=1}^{n} \tau_n(E_i^*), \tag{4}$$

where $E_{i+1}^* = E_i^* - \varepsilon_n$. Approximating the data $E_n^*(t_n)$ by an appropriate function, one gets a smooth "cooling-down curve" $E^*(t)$ which determines the time t_0 corresponding to E_0^* as well as the energy $E^*(t_0 + t_{\rm del})$ remaining in the system after a given time interval $t_{\rm del}$. By variation of the value of $t_{\rm del}$ one can find an energy E_f^* which describes the observed fragment mass dispersions ($\sigma_{m\,\rm corr}$).

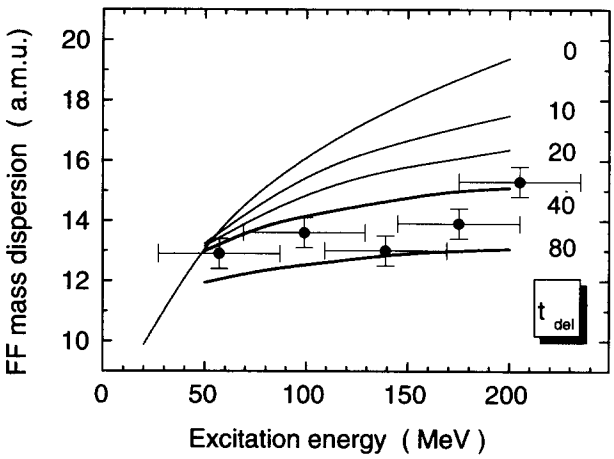

Fig. 5. Comparison of the experimental fission fragment (FF) mass dispersions ($\sigma_{m\,\mathrm{corr}}$; full circles) with some evaluations $\sigma_m(E*)$ (lines, see text) supposing different time intervals t_{del} (in units of 10^{-21} s).

Several curves evaluating the dependency $\sigma_m(E^*)$ for supposed values of t_{del} are shown in Fig. 5. The experimental dispersions ($\sigma_{m\,\mathrm{corr}}$) are well reproduced by t_{del} between 40×10^{-21} s and 80×10^{-21} s within the entire interval of E^* investigated. From our data we estimated a mean cooling (or fission delay) time at $t_{\mathrm{del}} = (60\pm20)\times10^{-21}$ s. This value is comparable with the scission time (t_{sci}) obtained by Hinde et al. [8], although, following the arguments given in the discussion above, t_{sci} should be slightly larger than t_{del}.

6. Summary

A quantitative analysis of the fragment mass dispersion for binary symmetric fission of the hot compound systems created by incomplete fusion of ^{7}Li with ^{232}Th at an energy of 43A MeV has been performed. Special efforts were made to exclude possible sources of systematic errors which can strongly influence the deduced fragment mass spectra.

For an interpretation of the unexpected small fragment mass dispersions observed for a nucleus near Th at excitation energies $E^* \geqslant 100$ MeV, we introduced a cooling time (t_{del}) during which the compound nucleus rapidly evaporates neutrons and, at the same time, loses a considerable amount of its initial excitation energy before it disintegrates by fission.

We understand the time t_{del} as a further possibility to estimate the dynamical time scale of the fission process at low intermediate energies with an uncertainty of less than 50%. The small fragment mass dispersions should be a direct consequence of the delayed course of fission governed by the dynamics of this large-scale collective motion. Although the initial excitation energy is doubled within the energy interval investigated, the highly heated compound nucleus succeeds to cool down fast before scission due

to the exponential decrease of the neutron evaporation time (τ_n) with increasing initial temperature (T) of the system: $\tau_n \sim \exp(-2aT)$. This might be the reason that the fission fragment mass dispersion shows a plateau-like behaviour at excitation energies in excess of ≈ 70 MeV.

Consequently, it seems that the stage in the course of the fission process when the primary fragment mass distribution is formed can be characterized by a nearly constant effective temperature $\Theta \approx 1.4$ MeV (corresponding to $E_f^* \approx 50$ MeV) over the entire interval of the initial excitation energy considered. The value of Θ is considerably lower than the initial temperature of the compound nucleus $T \approx 2$–3 MeV. Hence, at the suggested plateau $\sigma_m(E_f^*)$, the dispersion of the fission fragment mass distribution becomes a "delayed thermometer" not reproducing T.

Since the energy E_f^* found for reasonable values of t_{del} is close to the excitation energy E_{sci}^* remaining at scission, the formal application of Eq. (1) for the description of σ_m at $E^* \geqslant 100$ MeV requires the assumption that the effective stiffness parameter q_{eff} is smaller than q_{sci}. The supposition that the fragment mass distribution at these E^* is formed "well before" scission can, therefore, be understood only in this context. The used parameter q_{eff} had already to be introduced for the description of σ_m at $E^* < 100$ MeV [7], accounting in this way for the descent from the saddle to scission (i.e. $q_{\mathrm{eff}} > q_{\mathrm{sad}}$), but the temperature Θ taken in Ref. [7] is close to the initial temperature T. The "multi-chance" fission scenario implied by the statistical model and valid at lower excitation energies seems to find its limitations at E^* in excess of ≈ 70 MeV due to the rapid decrease of τ_n. The fission process becomes explicitly delayed (t_{del}) with respect to neutron evaporation. Considering the values obtained for E_f^* and t_{del}, one can therefore conclude that at these initial excitation energies the mass distribution of the primary fission fragments is indeed formed after a considerable energy release of the system due to particle emission, and the supposition of a constant effective stiffness parameter (q_{eff}) might be understood as a first-order approximation. Definite statements should only be possible by a multi-dimensional dynamical treatment of the fission process including the interplay with particle emission.

References

[1] D. Hilscher and H. Rossner, Ann. Phys. (Paris) 17 (1992) 471.
[2] M.G. Itkis, V.N. Okolovich, A.Ya. Rusanov and G.N. Smirenkin, Sov. J. Part. Nucl. 19 (1988) 301.
[3] G.D. Adeev, I.I. Gonchar, V.V. Pashkevich, N.I. Pischasov and O.I. Serdyuk, Sov. J. Part. Nucl. 19 (1988) 529.
[4] V.M. Strutinsky, Sov. J. Exp. Theo. Phys. 45 (1963) 1900.
[5] W.D. Myers and W.J. Swiatecki, Ark. Fys. 36 (1967) 343.
[6] W.D. Myers, Droplet Model of Atomic Nuclei (Plenum Press, New York, 1977).
[7] S.A. Karamyan, Yu.Ts. Oganesyan and B.I. Pustylnik, Sov. J. Nucl. Phys. 11 (1970) 546.
[8] D.J. Hinde, D. Hilscher, H. Rossner, B. Gebauer, M. Lehmann and M. Wilpert, Phys. Rev. C 45 (1992) 1229.
[9] D.J. Hinde, Nucl. Phys. A 553 (1993) 255c.
[10] T. Wada, Y. Abe and N. Carjan, Phys. Rev. Lett. 70 (1993) 3538.
[11] I.I. Gontchar, Phys. Elem. Part. At. Nucl. 26 (1995) 932.
[12] H. Delagrange, C. Gregoire, F. Scheuter and Y. Abe, Z. Phys. A 323 (1986) 437.

[13] Y. Abe, S. Ayik, P.-G. Reinhard and E. Suraud, Phys. Rep. 275 (1996) 49.
[14] T. Wada, Proc. Second Tours Symp. on Nucl. Phys., Tours, France, 1994;
Y. Abe, Proc. Third IN3P3-RIKEN Symp. on Heavy Ion Collisions, Tokyo, Japan, 1994.
[15] G. Casini, P.R. Maurenzig, A. Olmi and A.A. Stefanini, Nucl. Instr. and Meth. A 277 (1989) 445.
[16] E. Weissenberger, P. Geltenbort, A. Oed, F. Gönnenwein, and H. Faust, Nucl. Instr. and Meth. A 248 (1986) 506.
[17] G.G. Gulbekian and V. B. Kutner, Proc. FOBOS Workshop '94, Cracow, Poland, 1994, ed. W. Wagner (FZR-65, Rossendorf, 1995) p. 25.
[18] H.-G. Ortlepp, W. Wagner, C.-M. Herbach, A.A. Aleksandrov, I.A. Aleksandrova, M. Andrassy, A. Budzanowski, B. Czech, M. Danziger, L. Dietterle, V.N. Doronin, S. Dshemuchadse, A.S. Fomichev, W.D. Fromm, M. Gebhardt, P. Gippner, K. Heidel, Sh. Heinitz, H. Homeyer, S.A. Ivanovsky, D.V. Kamanin, I.V. Kolesov, A. Matthies, D. May, S.I. Merzlyakov, W. von Oertzen, Yu.Ts. Oganessian, G. Pausch, Yu. E. Penionzhkevich, Yu. V. Pyatkov, S.V. Radnev, G. Renz, L.A. Rubinskaya, I.D. Sandrev, K.D. Schilling, W. Seidel, D.I. Shishkin, A.P. Sirotin, H. Sodan, O.V. Strekalovsky, V.G. Tishchenko, V.V. Trofimov, I.P. Tsurin, C. Umlauf, D.V. Vakatov, V.M. Vasko, V.A. Vitenko, E. Will, M. Wilpert, R. Yanez, V.E. Zhuchko, P. Ziem and L. Zrodlowski, Nucl. Instr. and Meth. A 403 (1998) 65.
[19] A.A. Aleksandrov, I.A. Aleksandrova, M. Andrassy, L. Dietterle, V.N. Doronin, P. Gippner, C-M. Herbach, S.A. Ivanovsky, D.V. Kamanin, A. Matthies, D. May, H.-G. Ortlepp, G. Pausch, Yu. E. Penionzhkevich, G. Renz, K.D. Schilling, D.I. Shishkin, O.V. Strekalovsky, V.V. Trofimov, I.P. Tsurin, C. Umlauf, D.V. Vakatov, V.M. Vasko, W. Wagner, and V.E. Zhuchko, Proc. 5th Int. Conf. on Nucleus–Nucleus Collisions, Taormina, Italy, 1994, ed. M. Di Toro, E. Migneco, P. Piattelli, Nucl. Phys. A 583 (1994) 465c.
[20] C.-M. Herbach, Proc. FOBOS Workshop '94, Cracow, Poland, 1994, ed. W. Wagner (FZR-65, Rossendorf, 1995) p. 87.
[21] H.-G. Ortlepp, W. Wagner, A.A. Aleksandrov, I.A. Aleksandrova, M. Andrassy, L. Dietterle, V.N. Doronin, S. Dshemuchadse, P. Gippner, C.-M. Herbach, S.A. Ivanovsky, D.V. Kamanin, A. Matthies, G. Pausch, Yu. E. Penionzhkevich, G. Renz, K.D. Schilling, D.I. Shishkin, O.V. Strekalovsky, V.V. Trofimov, I.P. Tsurin, C. Umlauf, D.V. Vakatov, V.M. Vasko and V.E. Zhuchko, *in* Low Energy Nuclear Dynamics, ed. Yu. Oganessian, R. Kalpakchieva and W. von Oertzen (World Scientific, Singapore, 1995) p. 231.
[22] V.E. Viola, Jr., B.B. Back, K.L. Wolf, T.C. Awes, C.K. Gelbke, and H. Breuer, Phys. Rev. C 26 (1982) 178.
[23] M. Conjeaud, S. Harar, M. Mostefai, E.C. Pollacco, C. Volant, Y. Cassagnou, R. Dayras, R. Legrain, H. Oeschler and F. Saint-Laurent, Phys. Lett. B 159 (1985) 244.
[24] C. Gregoire and F. Scheuter, Phys. Lett. B 146 (1984) 21.
[25] G. Klotz-Engmann, H. Oeschler, J. Stroth, E. Krankeleit, Y. Cassagnou, M. Conjeaud, R. Dayras, S. Harar, R. Legrain, E.C. Pollacco and C. Volant, Nucl. Phys. A 499 (1989) 392.
[26] E.C. Pollacco, M. Conjeaud, S. Harar, C. Volant, Y. Cassagnou, R. Dayras, R. Legrain, M.S. Nguyen, H. Oeschler and F. Saint-Laurent, Phys. Lett. B 146 (1984) 29.
[27] D.J. Hinde, M. Dasgupta, J.R. Leigh, J.C. Mein, C.R. Morton, J.O. Newton and H. Timmers, Phys. Rev. C 53 (1996) 1290.
[28] R. Yanez, Forschungszentrum Rossendorf, private communication (see also R. Yanez, FZR-192, Rossendorf, 1997).
[29] W. Bauer, Phys. Rev. C 40 (1989) 715.
[30] A.Ya. Rusanov, M.G. Itkis and V.N. Okolovich, Yad. Fiz. 60 (1997) 773.
[31] P. Fröbrich and I.I. Gontchar, Nucl. Phys. A 563 (1993) 326.
[32] L.G. Moretto, Nucl. Phys. A 180 (1972) 337.